Geoderma 430 (2023) 116355

Contents lists available at ScienceDirect

Geoderma

journal homepage: www.elsevier.com/locate/geoderma

Volatile organic compound release across a permafrost-affected peatland

Yi Jiao [a], Cleo L. Davie-Martin [a,b], Magnus Kramshøj [a,b], Casper T. Christiansen [a,b], Hanna Lee [c,d], Inge H.J. Althuizen [d], Riikka Rinnan [a,b,*]

[a] Terrestrial Ecology Section, Department of Biology, University of Copenhagen, Universitetsparken 15, DK-2100 Copenhagen Ø, Denmark
[b] Center for Permafrost (CENPERM), Department of Geosciences and Natural Resource Management, University of Copenhagen, Øster Voldgade 10, DK-1350 Copenhagen K, Denmark
[c] Department of Biology, Norwegian University of Science and Technology (NTNU), NO-7491 Trondheim, Norway
[d] NORCE Norwegian Research Centre, Bjerknes Centre for Climate Research, Nygårdsgaten, 112, 5008 Bergen, Norway

ARTICLE INFO

Handling Editor: Jan Willem Van Groenigen

Keywords:
Arctic
Permafrost thaw
Peatland
Palsa
Climate change
VOCs

ABSTRACT

As the permafrost region experiences unprecedented climate warming, accelerated decomposition rates are potentially switching these cold landscapes to a hotspot of carbon emissions. In addition to the more widely studied greenhouse gases, carbon dioxide and methane, permafrost-affected soils may also be a source of volatile organic compounds (VOCs), but these reactive trace gases have so far received little attention. Nevertheless, VOCs can i) prolong the lifetime of atmospheric methane, ii) contribute to hazardous ozone production, and iii) lead to the formation of secondary organic aerosols. Consequently, changing VOC emissions may exert significant impacts on climate forcing factors that can both exacerbate or mitigate future climate change. Here, we conducted in situ measurements of soil and pond VOC emissions across an actively degrading permafrost-affected peatland in subarctic Norway. We used a permafrost thaw gradient as a space-for-time substitute that covered bare soil and vegetated peat plateaus, underlain by intact permafrost, and increasingly degraded permafrost landscapes: thaw slumps, thaw ponds, and vegetated thaw ponds. Results showed that every peatland landscape type was an important source of atmospheric VOCs, emitting a large variety of compounds, such as methanol, acetone, monoterpenes, sesquiterpenes, isoprene, hydrocarbons, and oxygenated VOCs. VOC composition varied considerably across the measurement period and across the permafrost thaw gradient. We observed enhanced terpenoid emissions following thaw slump degradation, highlighting the potential atmospheric impacts of permafrost thaw, due to the high chemical reactivities of terpenoid compounds. Higher VOC emission rates were observed in summer (June, July and August) compared to early autumn (September). Overall, our study demonstrates that VOCs are being emitted in significant quantities and with largely similar compositions upon permafrost thawing, inundation, and subsequent vegetation development, despite major differences in microclimate, hydrological regime, vegetation, and permafrost occurrence.

1. Introduction

Permafrost-affected peatlands occur in the sporadic discontinuous and continuous permafrost zones. In these peatlands, formation of ice-rich permafrost historically elevated the ground above the water table, establishing raised peat plateaus called “palsa”. The palsas have natural life cycles of degrading and forming (Seppälä, 1986). At the same time, ice-rich permafrost landscapes are particularly prone to climate warming, which increases the rate of thaw and degradation of these permafrost palsa peatlands, and the formation of new palsas is gravely reduced (Borge et al., 2017; Olvmo et al., 2020). The thaw of these permafrost-affected peatlands leads to excess ice melt and the overlying ground collapses into waterlogged thermokarst landforms. This drastically alters soil thermal and hydrological properties while disrupting vegetation and soil structure. This is a concern because permafrost-affected peatlands store an estimated 333–547 Pg C (Hugelius et al., 2014) and the changes in microclimate potentially drive production and release of greenhouse gases, such as carbon dioxide (CO_2) and methane (CH_4), into the atmosphere (Knoblauch et al., 2021; Natali et al., 2019).

Volatile organic compounds (VOCs) are a group of highly reactive

* Corresponding author at: Terrestrial Ecology Section, Department of Biology, University of Copenhagen, Universitetsparken 15, DK-2100 Copenhagen Ø, Denmark.
E-mail address: riikkar@bio.ku.dk (R. Rinnan).

https://doi.org/10.1016/j.geoderma.2023.116355
Received 26 August 2022; Received in revised form 12 January 2023; Accepted 19 January 2023
Available online 27 January 2023

gaseous carbon compounds with multiple climatic consequences when released into the atmosphere. For example, i) VOCs are susceptible to oxidation by atmospheric hydroxyl radicals (•OH), a process that will compete with the atmospheric oxidation of CH_4, thus extending the lifetime and global warming potential of CH_4 (Lelieveld et al., 2008; Peñuelas and Staudt, 2010); ii) The photochemical reactions between VOCs and NOx can produce hazardous tropospheric ozone (Atkinson, 2000); and iii) VOCs also contribute to aerosol formation and cloud condensation nuclei growth, which scatters the sunlight and affects the Earth's radiation balance (Hallquist et al., 2009; Petäjä et al., 2021). In comparison to the more widely studied CO_2 and CH_4 responses to climate warming, little attention has been paid to VOCs, although a few laboratory incubations have shown that a fraction of the stored organic carbon in permafrost and the upper active layer is indeed released into the atmosphere as VOCs (Kramshøj et al., 2019, 2018; Li et al., 2020). VOC emissions provide numerous feedbacks to climate warming of an unknown directions and magnitudes, which remain some of the greatest uncertainties in our understanding of the climate system (Schmale et al., 2021). The climatic consequences with respect to permafrost VOC emissions may be especially important in high-latitude regions where anthropogenic and vegetation VOC sources are otherwise largely absent.

Greenhouse gas exchange have been extensively studied in relation to permafrost thaw (e.g., Dorrepaal et al., 2009; Knoblauch et al., 2021; Łakomiec et al., 2021; Natali et al., 2019; Trucco et al., 2012), while in situ soil VOC emissions from permafrost-affected soils remain largely unknown. Nevertheless, there are two identified sources of VOCs in permafrost-affected soils: i) accumulative VOC storage released from within the soil pores directly and ii) newly synthesized VOCs from thaw-induced microbial decomposition of soil organic matter (Kramshøj et al., 2019, 2018; Li et al., 2020). On the other hand, microbes within the seasonally thawed upper organic horizon can also act as a sink of VOCs emitted from deeper in the soil profile (Kramshøj et al., 2018; Rinnan and Albers, 2020), similar to methane oxidation occurring in dry soil horizons (Voigt et al., 2019). Microbial VOC consumption is believed to be ubiquitous across different ecosystems but it is poorly studied (Cleveland and Yavitt, 1997; Rinnan and Albers, 2020; Trowbridge et al., 2020). Therefore, we need in situ measurements of net soil-atmosphere VOC emissions to quantify the potential VOC source strength of landscapes affected by permafrost.

Generally, soil VOC composition and emission rates are dependent on soil organic matter content (Kramshøj et al., 2018; Li et al., 2020) and soil hydrological regimes, especially whether the soil is oxic or anoxic (Kramshøj et al., 2018, 2019). Whole plant-soil system measurements conducted in climate chambers also suggested that emission rates and compound compositions are strongly affected by ground water table levels (Faubert et al., 2010a, 2011). The northern permafrost region spans a wide range of environments with large variations in soil organic matter content (Ping et al., 2008; Strauss et al., 2012) and moisture regimes (Lawrence et al., 2015; Sannel and Kuhry, 2011), which likely leads to differences in VOC composition and emission rates between distinct landscape types. Yet, we know very little about these potentially important sources of VOCs.

Overall, VOC emissions from permafrost-affected peatlands are a poorly quantified component of the global carbon cycle with potential climate feedbacks. Here, we quantified VOC emissions on permafrost thaw gradients of a permafrost-affected peat plateau transitioning towards a collapsed wetland, aiming to provide an understanding of the evolving VOC emissions from the natural life cycle of palsas as well as under climate change. We hypothesize that 1) permafrost-affected peatlands have significant soil VOC emissions to the atmosphere and that 2) permafrost thaw, leading to ground collapse and inundation, alters VOC emission rates and compositions.

2. Materials and methods

2.1. Site description

In situ sampling was carried out in a peatland complex in northern Norway near the Iškoras site (69.3°N, 25.3°E, 337 m a.s.L., Fig. 1a) from June to September of 2020. The peatland complex consists of several elevated peat plateaus, including intact and degrading permafrost areas, surrounded by wet fen, open mountain birch forest, and upland heath tundra. The site lies in the sporadic permafrost zone, has a mean annual temperature of –2.9 °C, and mean annual precipitation of 366 mm (1961–1990 climate normal values from nearest meteorological station on Iškorasfjellet; Kjellman et al., 2018). In recent years, the seasonally thawed active layer reached 50–70 cm in September, and the organic-rich peat soils extend down to about 1.5 m within the peat plateaus.

2.2. Permafrost thaw gradient

In 2017, we used naturally occurring landscape gradients of permafrost thaw and ground subsidence at our site to establish 30 plots in five distinct landscape types that are common features of degrading permafrost-affected peatlands. In this space-for-time substitution approach, our gradients represent dry, raised peat plateaus with intact permafrost (current conditions), permafrost degradation causing thaw slumping of palsas and formation of thermokarst thaw ponds (near future in years), and potential succession and vegetation establishment into these thaw ponds (future in decades or centuries).

We labelled landscape types underlain by intact permafrost "bare soil palsa" or "vegetated palsa". Areas with active permafrost degradation and ground subsidence were labelled "thaw slump", while "thaw pond" and "vegetated pond" labels represent complete permafrost thaw, subsidence, and inundation areas (Fig. 1b, c). Vegetated palsa plots were dominated primarily by evergreen shrubs (*Empetrum nigrum* ssp. *Hermaphroditum, Rhododendron tomentosum,* and *Andromeda polifolia)* and mosses and lichens, with few deciduous shrubs (*Betula nana, Vaccinium uliginosum*) and forbs (*Rubus chamaemorus)* present. Thaw slumps contained similar species but they had slightly different vegetation composition, which was dominated by mosses and lichens with forbs (*R. chamaemorus)*, and evergreen shrubs (*A. polifolia* and *E. nigrum* ssp. *Hermaphroditum)*. On the other hand, thaw ponds were dominated by *Sphagnum* mosses and sedges (*Carex rotundata* and *Eriophorum russeolum*). Bare soil palsas and thaw ponds lacked vegetation.

Six replicate transects were established, including each of the five landscape types (n = 6 per landscape type). We spread out the gradients to cover as much of the spatial variability of the peatland complex as possible, resulting in plots being situated up to 150 m apart.

2.3. VOC collection

VOCs were sampled from soil surfaces without vegetation using a push–pull headspace sampling system (Ortega and Helmig, 2008) from polyvinyl chloride (PVC) soil collars that had been installed to a soil depth of at least 10 cm in each plot three years prior to sampling, except for vegetated pond plots, which were established one year prior to sampling. The soil collars were placed in bare soil areas within each plot and any aboveground vascular plant biomass present was carefully removed within each soil collar, with this plant removal treatment repeated annually. The soil collars had a diameter of 11 cm and protruded above ground by ~ 10 cm, giving a headspace volume of ~ 1 L. For thaw pond and vegetated pond plots, we pre-drilled numerous small holes (⌀ = 1.5 cm) into the submerged collar part to ensure continuous water movement between collars and pond water. Custom-built press-fit lids containing two gas ports for the attachment of a Teflon inlet line and outlet vent were fitted to the soil collar. Battery-operated pumps were used to supply 230 mL min^{-1} of purified air to the soil collars, following passage through a PTFE membrane filter to remove particles, an

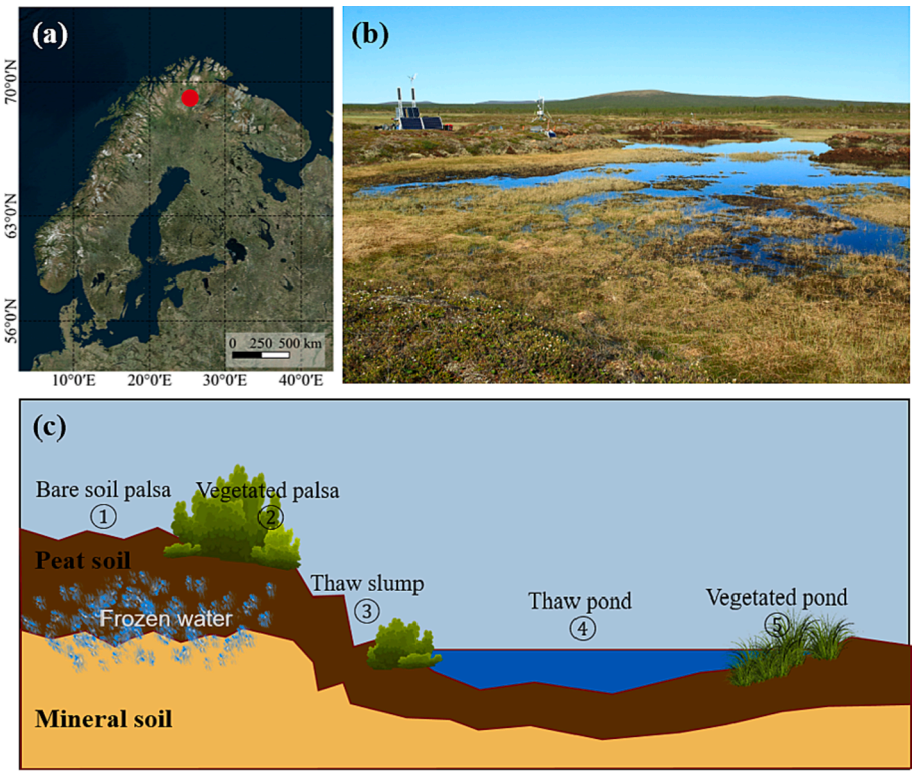

Fig. 1. (a) Location of the Iskoras peatland site in northern Norway, (b) a photo of the study site showing a peat plateau with intact permafrost, thaw slumping, thaw pond, and natural succession, and (c) a conceptual profile drawing of a transect containing the five landscape types, including intact bare soil palsa, intact vegetated palsa, thaw slump, thaw pond, and vegetated pond. Close-up photos of each landscape type are given in Figure S1.

activated charcoal filter to remove VOCs, and a potassium iodide-treated copper tube to remove ozone (Ortega and Helmig, 2008). The headspace of the soil collars was flushed with purified air for 5 min prior to measurements.

Two different two-bed stainless steel adsorbent cartridges i) hydrophobic 150 mg Tenax TA/200 mg Carbograph 1TD and ii) Tenax TA/Sulficarb carbonised molecular sieve (Markes International, Llantrisant, UK) were inserted in series into the outlet port of the soil collar lid and VOCs were sampled by drawing 200 mL min^{-1} through the cartridges for a period of 25 min. The hydrophobic cartridges were expected to reliably trap C_5-C_{30} compounds, whereas the back-up Sulficarb cartridges were used for collecting the lighter methanol and C_3-C_8 compounds that passed through the hydrophobic cartridge. After sampling, cartridges were capped and stored at 4 °C until analysis. It is noted that while methanol was measured, its concentrations are likely underrepresented because methanol is not effectively trapped by the adsorbents.

VOCs were collected once per plot during four sampling campaigns in 2020: 21–22 June (hereinafter referred to as "June"), 13–15 July ("July"), 8–11 August ("August"), and 3–4 September ("September"). Blank measurements were performed in each campaign in the same manner as described above using a separate 12 cm section of PVC collar. One end was capped with the same press-fit sampling lid and the base end was covered with a pre-cleaned polyethylene terephthalate oven bag (pre-cleaned at 120 °C for 1 h) and secured with an additional press-fit lid.

2.4. Microclimate during VOC measurements

Air temperature and relative humidity were monitored inside the soil collars with iButton dataloggers throughout sample collection (DS1923 Hygrochron, Maxim Integrated, San Jose, USA). Soil temperature and volumetric soil moisture content (ML3 ThetaProbe, Delta-T Devices ltd., Cambridge, UK) were measured in triplicate at a depth of 5 cm from within the plot area immediately adjacent to the soil collar, so as not to disturb the soil inside the collar (Table 1). Water temperature was recorded in the same manner in the thaw ponds.

Annual onsite meteorological records, such as air temperature, relative humidity, soil temperature, precipitation, snow depth and shortwave radiation, were retrieved from two meteorological stations close to the Iškoras site (Table S1).

2.5. VOC analysis

Analyses of VOC samples collected on adsorbent cartridges were performed using an Agilent gas chromatograph-mass spectrometer

Table 1
Summary of environmental conditions in the landscape type plots across the four measurement periods during the 2020 growing season showing the average (±S.E., n = 6). NA, data not available.

	June	July	August	September
Soil temperature [°C]				
Soil palsa	11.8 ± 0.6	11.6 ± 0.8	12.8 ± 0.8	8.69 ± 0.4
Vegetated palsa	12.4 ± 0.8	12.8 ± 0.7	14.0 ± 1.5	8.86 ± 0.5
Thaw slump	15.9 ± 1.5	14.6 ± 0.4	15.2 ± 1.4	9.79 ± 0.5
Thaw pond	17.7 ± 1.1	17.0 ± 0.8	16.2 ± 1.6	9.96 ± 0.4
Vegetated pond	15.8 ± 1.3	14.5 ± 0.7	15.4 ± 1.3	9.4 ± 0.2
Water temperature [°C]				
Thaw pond	19.4 ± 0.8	20.1 ± 0.9	NA	12.2 ± 1.2
Soil moisture content [%]				
Soil palsa	33.9 ± 2.4	32.7 ± 2.4	36.4 ± 3.4	33.7 ± 2.5
Vegetated palsa	17.9 ± 2.3	22.1 ± 3.0	23.4 ± 1.7	25.5 ± 2.7
Thaw slump	100.0 ± 0.0	100.0 ± 0.0	99.9 ± 0.1	95.5 ± 3.8
Thaw pond	100.0 ± 0.0	100.0 ± 0.0	100.0 ± 0.0	100.0 ± 0.0
Vegetated pond	100.0 ± 0.0	100.0 ± 0.0	100.0 ± 0.0	90.1 ± 7.2

(7890A GC – 5975C inert MSD, Santa Clara, USA). Adsorbent cartridges were thermally desorbed at 250 °C for 10 min (TD100-xr, Markes International, Llantrisant, UK), cryofocused at 10 ℃, and transferred with a split flow of 10 mL min^{-1} to the GC–MS system by way of a capillary transfer line kept at 160 °C. An HP-5 capillary column (50 m × 0.2 mm × 0.33 μm, Agilent Technologies, Santa Clara, USA) was used for the separation of VOCs with a helium carrier gas flow of 1.2 mL min^{-1}. For the hydrophobic adsorbent cartridges, an initial oven temperature of 40 °C was held for 3 min, before ramping at 5 °C min^{-1} to 210 °C and again at 20 °C min^{-1} to 250 °C, with a final hold of 8 min and total runtime of 47 min. The oven program was adjusted slightly for the Sulficarb adsorbent cartridges to better separate the lower molecular weight compounds, with an initial oven hold of 4 min at 40 °C, followed by a ramp at 5 °C min^{-1} to 200 °C, then at 25 °C min^{-1} to 250 °C with a final hold of 8 min and total runtime of 46 min. The ion source and quadrupole temperatures were held at 230 and 150 °C, respectively. No-injection column blanks and empty stainless-steel cartridges (containing no adsorbent material) were run periodically alongside the samples to provide an indication of background contamination arising from the analytical system (e.g., siloxanes, phthalates).

VOC concentrations were quantified using authentic standards of known concentration (Table S2). Standards were prepared by injecting 4 μL of a mixture, containing ~ 4 μg mL^{-1} of each standard compound, onto pre-cleaned stainless steel adsorbent cartridges under a flow of helium (100 mL min^{-1} for 2 min). Separate standards were prepared in methanol, for use with the hydrophobic adsorbent cartridges, and for lower molecular weight solvents in water (e.g., methanol, acetone etc.), for use with the Sulficarb cartridges. Standard cartridges were analyzed by GC–MS in the same manner as samples and blanks, and were run in duplicate before and after each batch of 20–30 sample cartridges. Linear calibration curves (0–25 μg mL^{-1}) were prepared and run prior to the analysis of samples, to confirm the detector response was linear.

Chromatograms were analyzed using PARADISe software v. 3.90 (Johnsen et al., 2017). Compounds were identified using pure standards, where available, or tentatively identified by comparison against mass spectra in the 2014 NIST Mass Spectral Library. The tentative identity of unknown compounds was accepted when the NIST match factor (MF) was greater than 800 and the probability was greater than 30 %. Where these conditions were not met, a tentative compound class identity was accepted where the molecular formula of at least two of the top three matches with the NIST database had the same molecular formula, otherwise the unknown was classified as an oxygenated VOC (oVOC, when the top three matches against NIST suggested a molecular formula containing oxygen) or other VOC (when the top three NIST matches suggested variable elemental compositions). We identified 210 unique compound peaks in our chromatograms (Table S3), which were subsequently classified into one of the following compound groups: methanol, acetone, isoprene, monoterpenes (including oxygenated monoterpenes, oMTs), sesquiterpenes (including oxygenated sesquiterpenes), oVOCs, hydrocarbons, and other (including unclassified unknowns and compounds with various functional groups, such as halogens, sulfur, and/or nitrogen-containing species, that do not fit in the other groups listed). Compounds present in the empty cartridges and known contaminants arising from the analytical system (e.g., cyclosiloxanes) were excluded.

Quantification was achieved by comparison of peak areas between the samples and standards and the known mass of standard injected for each compound. For compounds without an authentic standard, quantification was achieved by comparison with the closest structurally related standard in our mixture (e.g., α-pinene for MTs, eucalyptol for oMTs, and toluene for benzenoids and other compounds) (Table S2).

2.6. VOC emission rate calculation

VOC concentrations in the blanks varied by sampling date and temperature. Samples were paired with blanks collected on the same date at the most similar temperature (where multiple blanks were collected per day) and blank subtractions were performed on the VOC concentrations. Subsequently, VOC emission rates (ER, μg $m^{-2}h^{-1}$) were calculated according to equation (1):

$$ER = \frac{(C_{out} - C_{in}) \bullet Q_{in}}{SA_{soil}} \quad (1)$$

where C_{out} (μg L^{-1}) is the concentration of VOCs in the sample outlet, C_{in} is the concentration of VOCs in the purified inlet air (assumed to be 0 μg/L), Q_{in} (L h^{-1}) is the inflow rate to the soil collars, and SA_{soil} is the soil surface area of the collars (0.008 m^2). The emission rates calculated for the hydrophobic and Sulficarb adsorbent cartridges were summed.

2.7. Statistical Analyses

Linear mixed modelling was used to analyze for the differences between the landscape types and sampling months, as well as their interaction effects, on the emission rates of the VOC groups/compounds, with IBM SPSS Statistics (Version 28.0.0.0; IBM Corp., Armonk, NY, USA). Among the factors, month (continuous, seasonal variable) and landscape type (discrete, spatial variable), and their interaction (month × landscape type) were selected as fixed factors, and transect and plot were chosen as random factors to account for the repeated measurements across the different transects and plots. Significant effects of the fixed factors or interactions were identified if p values were < 0.05. Multiple comparisons between different landscape types were performed using post-hoc Bonferroni tests. VOC data were log-transformed to conform to normal distribution and homogeneity of error variances.

To further assess how month and landscape type affected the compound compositions, the log-transformed and unit variance-scaled VOC data (percentages of the individual compounds of the total VOC emission rates) were subjected to a principal component analysis (PCA) using SIMCA 16.0.1 (Umetrics, Umeå, Sweden). The scores of the first three principle components (PCs) were then analyzed by the linear mixed modelling procedure in SPSS, as described above, to identify seasonal and spatial effects.

3. Results

3.1. Overview of soil VOC emissions across landscape types and months

All landscape types showed VOC emissions from the soil or pond water surface throughout the entire measurement period (Fig. 2). Linear mixed modelling showed that time of year (month) and landscape type had significant effects on the emission rates of the majority of the VOC groups and individual compounds, with negligible differences in seasonal variation between landscape types (no significant interaction effects) (Table 2).

We measured the largest total VOC emission rates in vegetated palsa plots, averaging (± S.E.) 260.9 ± 77.3 μg $m^{-2}h^{-1}$ across all months, which was significantly greater than the total VOC emissions in the vegetated ponds (88.5 ± 16.6 μg $m^{-2}h^{-1}$; $p < 0.05$, Bonferroni test) (Fig. 2). The total VOC emission rates from soil/vegetated palsa and thaw slump plots were also significantly higher than those from the vegetated ponds, while thaw ponds had intermediate emission rates.

Within the sampling period from June to September, we measured larger total VOC release rates in the summer months than in September, early autumn (Figure S2). The highest total VOC emission rates were observed in June (261.5 ± 50.0 μg $m^{-2}h^{-1}$) and the emissions in June-August samplings were significantly greater than the total VOC emission rates in September (54.5 ± 5.8 μg $m^{-2}h^{-1}$, $p < 0.05$).

In terms of VOC emission composition (Fig. 2), the major compounds included acetone, methanol, and isoprene, and the major groups included monoterpenes, sesquiterpenes, hydrocarbons, oxygenated and other VOCs. Oxygenated VOCs always comprised the largest fraction of the emission profiles across months within each landscape type, ranging from 54 % to 73 %, and also across landscape types within each month,

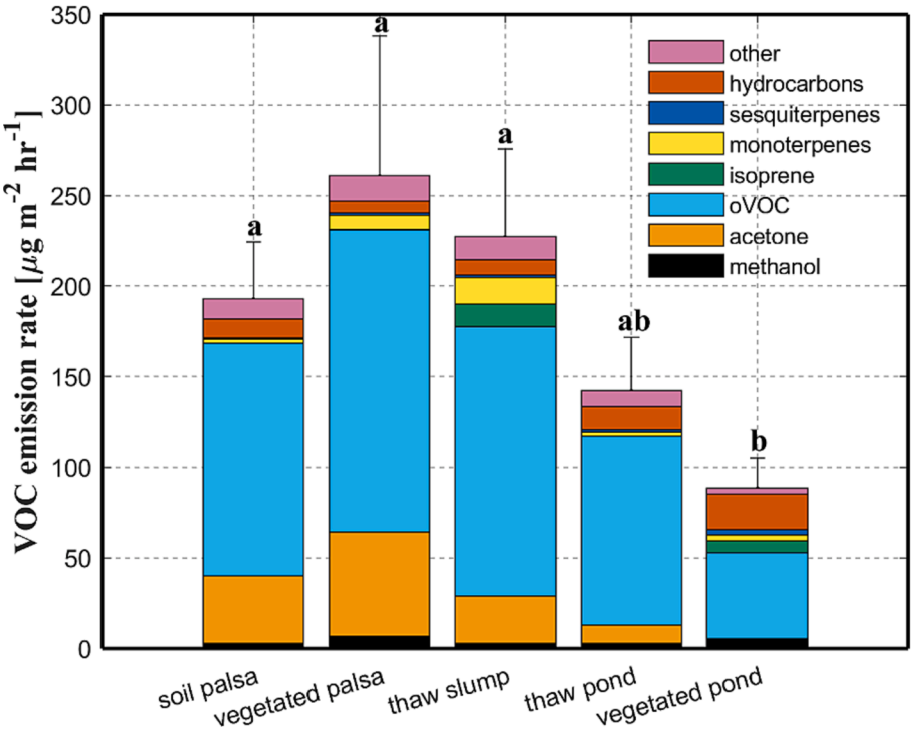

Fig. 2. Volatile organic compound (VOC) release from permafrost-affected peatland. Mean ± standard error (S.E.) emission rates of total VOCs (n = 24–29) stacked for the main compounds and groups grouped by landscape type, averaged across sampling months. Bars sharing a lower-case letter do not differ significantly ($p < 0.05$, Bonferroni test).

Table 2
Effects of month, landscape type, and their interaction on permafrost-affected peatland VOC emission rates and composition (described by principle components, PC 1 and 2 in Fig. 5), indicated by p-values for main effects and interactions from linear mixed models. Significant p-values appear in bold.

VOC	Month	Landscape type	Month × Landscape type
methanol	**<0.001**	0.942	0.88
acetone	0.46	**<0.001**	0.366
oVOCs	**<0.001**	**0.007**	0.643
isoprene	**0.004**	**<0.001**	0.086
monoterpenes	**<0.001**	**0.002**	1
sesquiterpenes	**<0.001**	**0.043**	0.767
hydrocarbons	0.58	0.93	0.803
other	**<0.001**	**0.002**	0.766
total VOCs	**<0.001**	**<0.001**	0.341
PC 1	**<0.001**	**0.008**	0.845
PC 2	**0.033**	**0.002**	0.497

ranging from 46 % to 70 % (Table S4). The dominant compounds in the oxygenated VOC group included 2,4-pentanedione ($C_5H_8O_2$), 2-methyl-2-propanol ($C_4H_{10}O$), 2,4-dimethylfuran (C_6H_8O), and 2,5-hexanedione ($C_6H_{10}O_2$) (see Table S3 for a complete list of individual compounds and their emission rates). Acetone and hydrocarbons represented the second most abundant fractions of the emission profiles. For example, hydrocarbons accounted for 9 % to 22 % of the thaw pond and vegetated pond emission profiles, while acetone accounted for 12 % and 24 % of the VOCs emitted in bare soil and vegetated palsas, respectively.

3.2. *Effect of landscape type on emission rates of specific VOC groups*

Acetone was emitted at lower rates in the vegetated ponds than all other landscape types (Fig. 3a; $p < 0.05$). Acetone emissions were also significantly lower from thaw ponds than soil palsa plots. In general, terpenoids exhibited higher emission rates from thaw slumps compared to other landscape types. For isoprene, thaw slumps and vegetated ponds had significantly higher emission rates than all other landscape types (Fig. 3b; $p < 0.05$). For monoterpenes, the emissions from thaw slumps were significantly higher than those from soil palsa, thaw pond and vegetated pond plots. For oxygenated and other VOC groups, vegetated ponds had lower emission rates compared to soil and vegetated palsa as well as thaw slump landscape types (Fig. 3c; $p < 0.05$). We observed no differences in methanol, sesquiterpenes, or hydrocarbon emission rates between any landscape types.

3.3. *Effect of month on emission rates of specific VOC groups*

For methanol, the highest emissions were recorded in June, when the emission rates were at least sixfold higher than in other months (Fig. 4a; $p < 0.05$). For acetone, June also showed the highest emission rates, but the differences between months were not significant.

Among the terpenoids, isoprene exhibited significantly lower emission rates in September than in all other months (Fig. 4b; $p < 0.05$). Similarly, the lowest emission rates of monoterpenes were also observed in September and were significantly lower than the monoterpene emissions in August ($p < 0.05$). For sesquiterpenes, significantly lower emission rates were observed in September, in comparison to June and August ($p < 0.05$), while July emission rates were lower than June ($p < 0.05$). For oVOCs and other VOCs, September showed significantly lower emission rates than all other months (Fig. 4c and 4d; $p < 0.05$), while there were no significant seasonal differences in hydrocarbon emission rates.

3.4. *Seasonal and spatial effects on VOC composition profiles*

Principal component analysis of the percent contributions of the individual VOCs further revealed the seasonal and spatial effects on the VOC profiles (Fig. 5). The first PC, which explained 29.0 % of the variance, and the second PC, which explained 10.8 % of the variance, both differed significantly among landscape types and months (Table 2). The vegetated pond profiles were clearly separated from the other

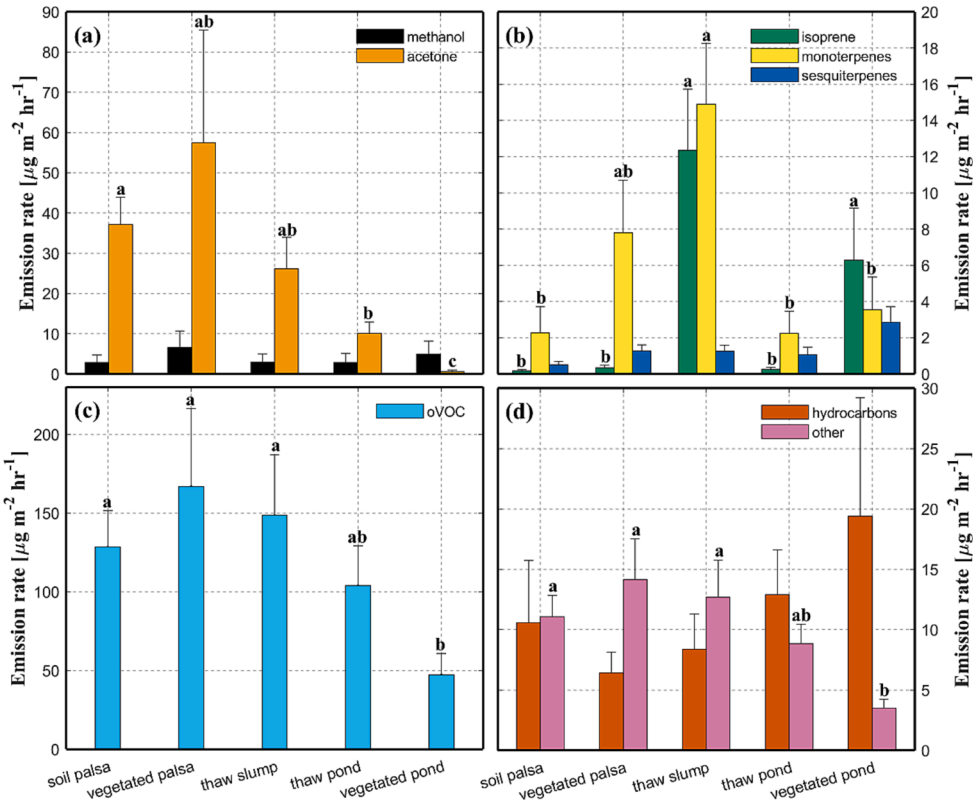

Fig. 3. Volatile organic compound (VOC) emission rates from permafrost-affected peatland across different landscape types. The bars represent the mean ± S.E. of VOC emission rates (n = 19–24). The black dashed line separates the landscape types by intact palsas and degraded permafrost (thaw slump and thaw ponds). Within a compound/VOC group, bars sharing a lower-case letter do not differ significantly ($p < 0.05$, Bonferroni test). There were no significant differences between landscape types for methanol, sesquiterpenes, or hydrocarbons.

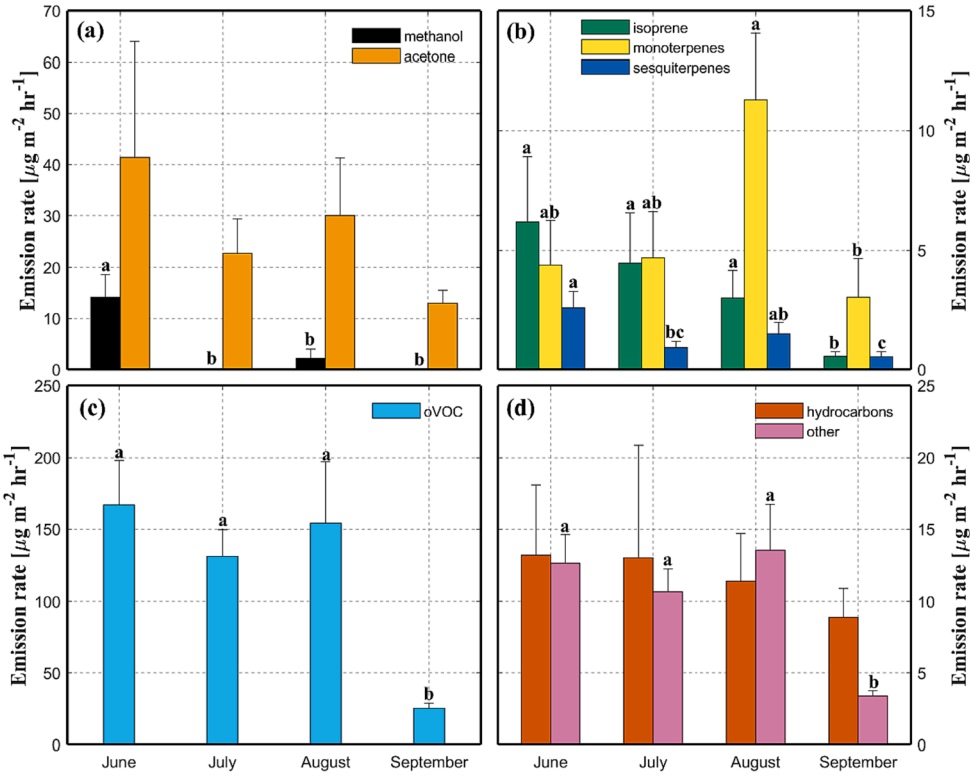

Fig. 4. Monthly emission rates of volatile organic compounds (VOCs) released from permafrost-affected peatland. The bars represent the mean ± S.E. of VOC emission rates (n = 28–29). Within a compound/VOC group, bars sharing a lower-case letter do not differ significantly ($p < 0.05$, Bonferroni test). There were no significant differences between months for acetone and hydrocarbons.

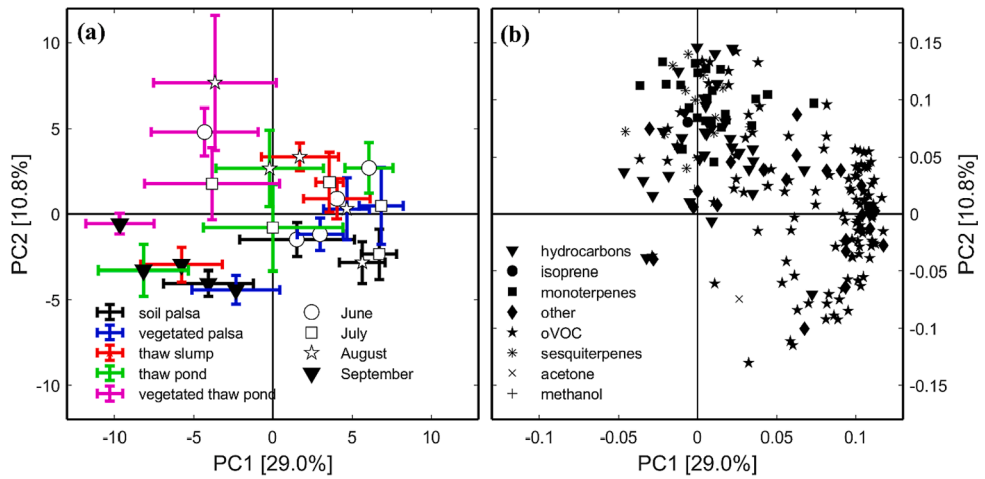

Fig. 5. Principle component analysis of the emission profiles with 210 volatile organic compounds (VOCs). (a) Scores (mean ± S.E., n = 6) for each month and landscape type in PC1 and PC2, and (b) the corresponding loadings for the VOCs symbol-coded by group. Variances explained by the PCs are provided in square brackets.

landscape types, with the lowest scores on PC1 and the highest scores on PC2 (Fig. 5a; $p < 0.05$, Bonferroni test). The palsa landscape types exhibited relatively similar VOC profiles and partially overlapped with the thaw slump profiles. The thaw pond profiles fell in between the intact palsa and thaw slump landscape types and the vegetated ponds. The VOC profiles within any given landscape type were relatively similar between the different months, except for September, which grouped together regardless of the landscape type, exhibiting the lowest scores on PC1 and PC2.

The loading plot showed that a large majority of VOCs had high loadings on PC1, describing the high emissions in June-July samples and palsa landscape types (Fig. 5b). The emissions from vegetated thaw ponds were characterized by certain hydrocarbons (e.g., hexane and toluene), an oVOC (acetophenone), and terpenoids (terpinolene and α-bisabolene). September samples were characterized by higher relative contributions from o-xylene and benzaldehyde than the other samples.

4. Discussion

Our results, featuring the first in situ measurements of soil VOC emissions from permafrost-affected peatlands, show that permafrost peatland landscape types are significant sources of VOCs into the atmosphere, with average emission rates ranging between 190 and 254 μg $m^{-2}h^{-1}$. The peatland soil continues to emit VOCs as it undergoes thaw slump degradation in response to warming (Turetsky et al., 2019), and also in the subsequent stages of inundation and sedge vegetation development, with emission rates ranging from 83.5 – 224 μg $m^{-2}h^{-1}$. The total VOC emission rates we report for this permafrost-affected peatland are comparable to, or higher than, other reported natural soil VOC sources, such as temperate and subarctic heath soils (Rinnan et al., 2013), subarctic mountain birch forest soil (Faubert et al., 2012).

VOC emissions exhibited large spatial and seasonal (i.e., summer and early autumn) variations across the different sampling months and landscape types, suggesting that VOC emissions from permafrost-affected peatland soils are regulated by multiple factors. Instead of a simple temperature-dependent or moisture-regulated relationship, the environmental dependencies of VOC-releasing and consuming processes could mask any correlations to the emissions. In addition, VOCs may originate from both accumulated gases escaping from the soil pores upon thawing and from microbially mediated production from the organic matter (Kramshøj et al., 2019; Li et al., 2020).

On the spatial scale, lower emission rates of total VOCs were observed from thaw ponds and vegetated ponds compared to the intact palsas and thaw slumps. High water table and waterlogged soil conditions may result in higher VOC emissions, due to enhanced organic matter fermentation, in addition to inhibited VOC consumption under anoxic conditions (Kramshøj et al., 2019; Rinnan and Albers, 2020). However, lower emission rates from thaw ponds and vegetated ponds were found in almost all compounds/VOC groups, except for hydrocarbons and sesquiterpenes. This may be due to that the standing water table on top of soil inhibited or slowed down the diffusive transport of VOCs to the atmosphere (Kramshøj et al., 2019; Zhao et al., 2016). In addition, VOCs such as methanol, acetone, and oVOCs display water solubility-two to three magnitudes higher than that of hydrocarbons (Hakkim et al., 2019; Weidenhamer et al., 1993). Hence, the dissolution of VOCs with higher solubility may be another reason for the observed lower VOC emissions and the bias across different groups for the ponds relative to the soil surfaces. Although permafrost thaw is projected to increase soil dryness in some areas (Teufel and Sushama, 2019), land surface subsidence in lowland permafrost areas could initially lead to inundation (Avis et al., 2011), for example, thermokarst landscapes and the formation of thaw slump and thaw ponds in degrading permafrost-affected peatlands (Faubert et al., 2010a; IPCC, 2021; Turetsky et al., 2019, 2020). Such processes may reduce VOC emission rates, thereby alleviating their atmospheric effects. Nevertheless, VOC emission may increase in the long term due to the soil dryness.

Throughout the sampling period, consistently lower VOC emission rates and clearly distinct compound compositions were observed in September compared to the June-August measurements. This may be due to the lower temperatures during the September sampling period, as well as seasonal plant phenology associated changes in the ecosystem leading to lower emission rates at this time (Table 1). Data from other tundra ecosystems, and a subarctic non-permafrost peatland, show that VOC emission rates often decline during August even though air temperatures remain at a similar level as earlier in the summer (Faubert et al., 2010a,b). While plant senescence likely drives the autumnal decline of VOC emissions from plant-soil-systems, interactions with soil processes, e.g., via root exudation, can also play a role (Williams and Yavitt, 2010).

By combining two complementary types of adsorbent cartridges, we could sample and separate a variety of compounds, including methanol, acetone, and isoprene, as well as compounds grouped into monoterpenes, sesquiterpenes, hydrocarbons, oxygenated and other VOCs. Our methanol emission rates were comparable to those of a temperate ponderosa pine forest soil measured previously using proton-transfer-reaction mass spectrometry (PTR-MS) (Greenberg et al., 2012). However, acetone emissions in our study were up to 14 times higher than those of the ponderosa pine forest soil (Greenberg et al., 2012) and

comparable to acetone emissions from a temperate agricultural (cereal) soil (Schade and Custer, 2004). Monoterpene emission rates from our permafrost-affected peatland soil were comparable to Mediterranean oak forest soils (Asensio et al., 2007) and boreal pine forest soils (Aaltonen et al., 2011). These comparisons show that permafrost-affected peatland landscapes are significant sources of VOCs to the atmosphere. This is especially relevant in the high latitudes, which have low plant biomass and therefore, the relative importance of soil VOC sources is likely high compared to vegetation sources.

Palsa peatlands in the Arctic thaw and collapse naturally (Seppälä, 1986). The Arctic warming (IPCC, 2021) may further accelerate this process (Borge et al., 2017; Olvmo et al., 2020). The organic matter stored is mobilized during permafrost thaw and active layer thickening (Biskaborn et al., 2019; Miner et al., 2022). Increased microbial activity due to rising temperatures also enhances the decomposition of these historical carbon deposits, leading to higher carbon release to the atmosphere in the form of CO_2, CH_4, and VOCs (Schuur et al., 2015). Thaw-derived permafrost collapse may expose the carbon deposits to decomposition faster and on larger scale, with subsequent carbon release to the atmosphere (Miner et al., 2022; Turetsky et al., 2020, 2019). Therefore, enhanced VOC emissions are expected due to the increasingly exposed surfaces of stored carbon and rising temperatures. Nevertheless, we did not observe enhanced total soil VOC emissions when comparing intact palsas (190–254 μg $m^{-2}h^{-1}$) to thaw slump degradation (224 μg $m^{-2}h^{-1}$). This could be due to the ample organic matter availability in peat regardless of the permafrost degradation status or due to VOC consumption processes changing simultaneously with VOC production (Rinnan & Albers, 2020), thus resulting in similar net emission rates.

Terpenoid emission rates (the sum of isoprene, monoterpenes and sesquiterpenes) were higher in thaw slump than in palsa plots, suggesting that permafrost thaw-related processes enhanced terpenoid emissions. Although terpenoids were not the major constituents (1.5–14.3 %) of the whole VOC profile emitted from the soil, they have a higher reactivity and aerosol yield than many other compounds, which makes terpenoid compounds relatively more important in atmospheric chemistry (Jaoui et al., 2013; Li et al., 2020). Plants, both aboveground vegetation and belowground roots, are usually regarded as an important biogenic source of terpenoids (Dudareva et al., 2004). Nevertheless, we observed much higher soil emission rates of terpenoids (48.9-, 3.0-, and 1.4-fold higher release for isoprene, monoterpenes, and sesquiterpenes, respectively) from the degrading thaw slump with less vegetation, compared to intact vegetated palsas. In the intact vegetated palsas, plant root VOC emissions could have had a higher contribution due to greater evergreen shrub biomass surrounding the measurement collars (Wester-Larsen et al., 2020), but the terpenoid emissions were lower that from the thaw slump. Hence, our study suggests that thawing permafrost landscapes, including the natural degrading of palsa peatlands, are a potential source of atmospheric terpenoids, which have documented atmospheric impacts, such as the production of hazardous tropospheric ozone (Atkinson, 2000) and secondary organic aerosols (Hallquist et al., 2009; Petäjä et al., 2021), thereby regulating radiative forcing in the remote Arctic regions.

In contrast to the terpenoids, emissions of the oVOCs, and especially those of acetone and methanol, decreased from the palsa landscape type with intact permafrost through the thaw slump towards thaw ponds. Acetone and methanol have been shown to be dominant permafrost thaw-related compounds in laboratory incubations using PTR-MS techniques (Kramshøj et al., 2018; Li et al., 2020); and our results – although based on adsorbent cartridge analysis rather than online analysis – support these findings. However, microbes in the active layer are capable of mineralizing acetone and methanol diffused from the permafrost thaw front underneath and convert these VOCs into CO_2 (Kramshøj et al., 2018). Indeed, increasing soil CO_2 and CH_4 emission rates are also observed in thaw slumps, relative to palsa plots, at the same field site (C. T. Christiansen *et al.*, in prep.), which may be partially attributed to the biodegradation of VOCs in the active layer. However, as our study quantified emission rates and did not separate VOC production and consumption processes, we cannot partition the contributions of these processes along the permafrost thaw gradient.

5. Conclusion

Our study demonstrates that permafrost-affected peatland landscapes are important sources of VOCs to the atmosphere. Using the space-for-time substitution approach, this study measured VOC emission rates from a thaw gradient continuum of a permafrost-affected peatland across different landscape types, and provided references to the projected VOC emission rates and compositions in a dynamic permafrost-affected peatland undergoing thaw and landscape degradation. Palsa collapse and formation of thaw slumps, both naturally and induced by climate warming, was associated with enhanced soil emissions of highly reactive terpenoids (e.g., isoprene, monoterpenes).

Our study highlights the potential atmospheric impact of VOC emissions from permafrost thaw and associated soils. These emissions need to be considered because of the limited anthropogenic VOC emissions from permafrost areas. This study also shows that VOC emissions from peatland landscapes were characterized by relatively large seasonal and spatial variabilities, emphasizing the complexity of the underlying VOC source and sink processes that can be influenced by soil degradation, soil water conditions, and vegetation development. Future studies should focus on understanding the processes and drivers involved in VOC emissions under permafrost thaw and seasonal variability.

Declaration of Competing Interest

The authors declare that they have no known competing financial interests or personal relationships that could have appeared to influence the work reported in this paper.

Data availability

Data is publicly available on Zenodo repository, DOI number is included in the data availability section of the paper.

Acknowledgment

This study was supported by European Research Council (ERC) under European Union's Horizon 2020 research and innovation program (TUVOLU, grant 771012 to R.R.), the Elite Research Prize of the Danish Ministry for Higher Education and Science to R.R. (grant 9095-00004), Danish National Research Foundation (Center for Permafrost, grant CENPERM DNRF100), and Research Council of Norway (EMERALD, grant 294948 to H.L.).

Author contributions

R.R. conceived of and secured funds for this study; H.L. and C.T.C. established the study site and its infrastructure in 2017; C.D-M., M.K., and R.R. designed the measurement plan and determined logistic and technical details, based upon which C.D-M., M.K., C.T.C., H.L., and I.A. conducted the fieldwork and collected the samples in 2020; C.D-M. analyzed the samples, processed the raw data, and wrote up relevant methodology; Y.J. completed the formal analysis, produced the map and figures, and prepared the manuscript with input from all authors, particularly C.D-M. and C.T.C.

Data availability statement

All data that support the findings of this study is presented in the manuscript and the supporting information. In addition, we have

archived the raw data and figure source data in online repository Zenodo at http://doi.org/10.5281/zenodo.6531553 with public access.

Appendix A. Supplementary data

Supplementary data to this article can be found online at https://doi.org/10.1016/j.geoderma.2023.116355.

References

Aaltonen, H., Pumpanen, J., Pihlatie, M., Hakola, H., Hellén, H., Kulmala, L., Vesala, T., Bäck, J., 2011. Boreal pine forest floor biogenic volatile organic compound emissions peak in early summer and autumn. Agric. For. Meteorol. Spec. Issue Atmos. Transp. Chem. For. Ecosyst. 151, 682–691. https://doi.org/10.1016/j.agrformet.2010.12.010.

Asensio, D., Peñuelas, J., Llusià, J., Ogaya, R., Filella, I., 2007. Interannual and interseasonal soil CO2 efflux and VOC exchange rates in a Mediterranean holm oak forest in response to experimental drought. Soil Biol. Biochem. 39, 2471–2484. https://doi.org/10.1016/j.soilbio.2007.04.019.

Atkinson, R., 2000. Atmospheric chemistry of VOCs and NOx. Atmos. Environ. 34, 2063–2101. https://doi.org/10.1016/S1352-2310(99)00460-4.

Avis, C.A., Weaver, A.J., Meissner, K.J., 2011. Reduction in areal extent of high-latitude wetlands in response to permafrost thaw. Nature Geosci 4, 444–448. https://doi.org/10.1038/ngeo1160.

Biskaborn, B.K., Smith, S.L., Noetzli, J., Matthes, H., Vieira, G., Streletskiy, D.A., Schoeneich, P., Romanovsky, V.E., Lewkowicz, A.G., Abramov, A., Allard, M., Boike, J., Cable, W.L., Christiansen, H.H., Delaloye, R., Diekmann, B., Drozdov, D., Etzelmüller, B., Grosse, G., Guglielmin, M., Ingeman-Nielsen, T., Isaksen, K., Ishikawa, M., Johansson, M., Johannsson, H., Joo, A., Kaverin, D., Kholodov, A., Konstantinov, P., Kröger, T., Lambiel, C., Lanckman, J.-P., Luo, D., Malkova, G., Meiklejohn, I., Moskalenko, N., Oliva, M., Phillips, M., Ramos, M., Sannel, A.B.K., Sergeev, D., Seybold, C., Skryabin, P., Vasiliev, A., Wu, Q., Yoshikawa, K., Zheleznyak, M., Lantuit, H., 2019. Permafrost is warming at a global scale. Nat. Commun. 10, 264. https://doi.org/10.1038/s41467-018-08240-4.

Borge, A.F., Westermann, S., Solheim, I., Etzelmüller, B., 2017. Strong degradation of palsas and peat plateaus in northern Norway during the last 60 years. Cryosphere 11, 1–16. https://doi.org/10.5194/tc-11-1-2017.

Cleveland, C.C., Yavitt, J.B., 1997. Consumption of atmospheric isoprene in soil. Geophys. Res. Lett. 24, 2379–2382. https://doi.org/10.1029/97GL02451.

Dorrepaal, E., Toet, S., van Logtestijn, R.S.P., Swart, E., van de Weg, M.J., Callaghan, T. V., Aerts, R., 2009. Carbon respiration from subsurface peat accelerated by climate warming in the subarctic. Nature 460, 616–619. https://doi.org/10.1038/nature08216.

Dudareva, N., Pichersky, E., Gershenzon, J., 2004. Biochemistry of plant volatiles. Plant Physiol. 135, 1893–1902. https://doi.org/10.1104/pp.104.049981.

Faubert, P., Tiiva, P., Rinnan, Å., Michelsen, A., Holopainen, J.K., Rinnan, R., 2010a. Doubled volatile organic compound emissions from subarctic tundra under simulated climate warming. New Phytol. 187, 199–208. https://doi.org/10.1111/j.1469-8137.2010.03270.x.

Faubert, P., Tiiva, P., Rinnan, Å., Räsänen, J., Holopainen, J.K., Holopainen, T., Kyrö, E., Rinnan, R., 2010b. Non-methane biogenic volatile organic compound emissions from a subarctic peatland under enhanced UV-B radiation. Ecosystems 13, 860–873. https://doi.org/10.1007/s10021-010-9362-1.

Faubert, P., Tiiva, P., Rinnan, Å., Räty, S., Holopainen, J.K., Holopainen, T., Rinnan, R., 2010c. Effect of vegetation removal and water table drawdown on the non-methane biogenic volatile organic compound emissions in boreal peatland microcosms. Atmos. Environ. 44, 4432–4439. https://doi.org/10.1016/j.atmosenv.2010.07.039.

Faubert, P., Tiiva, P., Nakam, T.A., Holopainen, J.K., Holopainen, T., Rinnan, R., 2011. Non-methane biogenic volatile organic compound emissions from boreal peatland microcosms under warming and water table drawdown. Biogeochemistry 106, 503–516. https://doi.org/10.1007/s10533-011-9578-y.

Faubert, P., Tiiva, P., Michelsen, A., Rinnan, Å., Ro-Poulsen, H., Rinnan, R., 2012. The shift in plant species composition in a subarctic mountain birch forest floor due to climate change would modify the biogenic volatile organic compound emission profile. Plant and Soil 352, 199–215. https://doi.org/10.1007/s11104-011-0989-2.

Greenberg, J.P., Asensio, D., Turnipseed, A., Guenther, A.B., Karl, T., Gochis, D., 2012. Contribution of leaf and needle litter to whole ecosystem BVOC fluxes. Atmos. Environ. 59, 302–311. https://doi.org/10.1016/j.atmosenv.2012.04.038.

Hakkim, H., Sinha, V., Chandra, B.P., Kumar, A., Mishra, A.K., Sinha, B., Sharma, G., Pawar, H., Sohpaul, B., Ghude, S.D., Pithani, P., Kulkarni, R., Jenamani, R.K., Rajeevan, M., 2019. Volatile organic compound measurements point to fog-induced biomass burning feedback to air quality in the megacity of Delhi. Sci. Total Environ. 689, 295–304. https://doi.org/10.1016/j.scitotenv.2019.06.438.

Hallquist, M., Wenger, J.C., Baltensperger, U., Rudich, Y., Simpson, D., Claeys, M., Dommen, J., Donahue, N.M., George, C., Goldstein, A.H., Hamilton, J.F., Herrmann, H., Hoffmann, T., Iinuma, Y., Jang, M., Jenkin, M.E., Jimenez, J.L., Kiendler-Scharr, A., Maenhaut, W., McFiggans, G., Mentel, T.F., Monod, A., Prévôt, A.S.H., Seinfeld, J.H., Surratt, J.D., Szmigielski, R., Wildt, J., 2009. The formation, properties and impact of secondary organic aerosol: Current and emerging issues. Atmos. Chem. Phys. 9, 5155–5236. https://doi.org/10.5194/acp-9-5155-2009.

Hugelius, G., Strauss, J., Zubrzycki, S., Harden, J.W., Schuur, E. a. G., Ping, C.-L., Schirrmeister, L., Grosse, G., Michaelson, G.J., Koven, C.D., O'Donnell, J.A., Elberling, B., Mishra, U., Camill, P., Yu, Z., Palmtag, J., Kuhry, P., 2014. Estimated stocks of circumpolar permafrost carbon with quantified uncertainty ranges and identified data gaps. Biogeosciences 11, 6573–6593. 10.5194/bg-11-6573-2014.

IPCC, 2021. Climate Change 2021: The Physical Science Basis. Contribution of Working Group I to the Sixth Assessment Report of the Intergovernmental Panel on Climate Change [Masson-Delmotte, V., P. Zhai, A. Pirani, S.L.Connors, C. Péan, S. Berger, N. Caud, Y. Chen, L. Goldfarb, M.I. Gomis, M. Huang, K. Leitzell, E. Lonnoy, J.B.R. Matthews, T.K. Maycock, T. Waterfield, O. Yelekçi, R. Yu, and B. Zhou (eds.)]. Cambridge University Press.

Jaoui, M., Kleindienst, T.E., Docherty, K.S., Lewandowski, M., Offenberg, J.H., Jaoui, M., Kleindienst, T.E., Docherty, K.S., Lewandowski, M., Offenberg, J.H., 2013. Secondary organic aerosol formation from the oxidation of a series of sesquiterpenes: α-cedrene, β-caryophyllene, α-humulene and α-farnesene with O3, OH and NO3 radicals. Environ. Chem. 10, 178–193. https://doi.org/10.1071/EN13025.

Johnsen, L.G., Skou, P.B., Khakimov, B., Bro, R., 2017. Gas chromatography – mass spectrometry data processing made easy. J. Chromatogr. A 1503, 57–64. https://doi.org/10.1016/j.chroma.2017.04.052.

Kjellman, S.E., Axelsson, P.E., Etzelmüller, B., Westermann, S., Sannel, A.B.K., 2018. Holocene development of subarctic permafrost peatlands in Finnmark, northern Norway. The Holocene 28, 1855–1869. https://doi.org/10.1177/0959683618798126.

Knoblauch, C., Beer, C., Schuett, A., Sauerland, L., Liebner, S., Steinhof, A., Rethemeyer, J., Grigoriev, M.N., Faguet, A., Pfeiffer, E.-M., 2021. Carbon Dioxide and Methane Release Following Abrupt Thaw of Pleistocene Permafrost Deposits in Arctic Siberia. Journal of Geophysical Research: Biogeosciences 126, e2021JG006543. 10.1029/2021JG006543.

Kramshøj, M., Albers, C.N., Holst, T., Holzinger, R., Elberling, B., Rinnan, R., 2018. Biogenic volatile release from permafrost thaw is determined by the soil microbial sink. Nat. Commun. 9, 3412. https://doi.org/10.1038/s41467-018-05824-y.

Kramshøj, M., Albers, C.N., Svendsen, S.H., Björkman, M.P., Lindwall, F., Björk, R.G., Rinnan, R., 2019. Volatile emissions from thawing permafrost soils are influenced by meltwater drainage conditions. Glob. Chang. Biol. 25, 1704–1716. https://doi.org/10.1111/gcb.14582.

Łakomiec, P., Holst, J., Friborg, T., Crill, P., Rakos, N., Kljun, N., Olsson, P.-O., Eklundh, L., Persson, A., Rinne, J., 2021. Field-scale CH_4 emission at a subarctic mire with heterogeneous permafrost thaw status. Biogeosciences 18, 5811–5830. https://doi.org/10.5194/bg-18-5811-2021.

Lawrence, D.M., Koven, C.D., Swenson, S.C., Riley, W.J., Slater, A.G., 2015. Permafrost thaw and resulting soil moisture changes regulate projected high-latitude CO 2 and CH 4 emissions. Environ. Res. Lett. 10, 094011 https://doi.org/10.1088/1748-9326/10/9/094011.

Lelieveld, J., Butler, T.M., Crowley, J.N., Dillon, T.J., Fischer, H., Ganzeveld, L., Harder, H., Lawrence, M.G., Martinez, M., Taraborrelli, D., Williams, J., 2008. Atmospheric oxidation capacity sustained by a tropical forest. Nature 452, 737–740. https://doi.org/10.1038/nature06870.

Li, H., Väliranta, M., Mäki, M., Kohl, L., Sannel, A.B.K., Pumpanen, J., Koskinen, M., Bäck, J., Bianchi, F., 2020. Overlooked organic vapor emissions from thawing Arctic permafrost. Environ. Res. Lett. 15, 104097 https://doi.org/10.1088/1748-9326/abb62d.

Miner, K.R., Turetsky, M.R., Malina, E., Bartsch, A., Tamminen, J., McGuire, A.D., Fix, A., Sweeney, C., Elder, C.D., Miller, C.E., 2022. Permafrost carbon emissions in a changing Arctic. Nat Rev Earth Environ 3, 55–67. https://doi.org/10.1038/s43017-021-00230-3.

Natali, S.M., Watts, J.D., Rogers, B.M., Potter, S., Ludwig, S.M., Selbmann, A.-K., Sullivan, P.F., Abbott, B.W., Arndt, K.A., Birch, L., Björkman, M.P., Bloom, A.A., Celis, G., Christensen, T.R., Christiansen, C.T., Commane, R., Cooper, E.J., Crill, P., Czimczik, C., Davydov, S., Du, J., Egan, J.E., Elberling, B., Euskirchen, E.S., Friborg, T., Genet, H., Göckede, M., Goodrich, J.P., Grogan, P., Helbig, M., Jafarov, E.E., Jastrow, J.D., Kalhori, A.A.M., Kim, Y., Kimball, J.S., Kutzbach, L., Lara, M.J., Larsen, K.S., Lee, B.-Y., Liu, Z., Loranty, M.M., Lund, M., Lupascu, M., Madani, N., Malhotra, A., Matamala, R., McFarland, J., McGuire, A.D., Michelsen, A., Minions, C., Oechel, W.C., Olefeldt, D., Parmentier, F.-J.-W., Pirk, N., Poulter, B., Quinton, W., Rezanezhad, F., Risk, D., Sachs, T., Schaefer, K., Schmidt, N.M., Schuur, E.A.G., Semenchuk, P.R., Shaver, G., Sonnentag, O., Starr, G., Treat, C.C., Waldrop, M.P., Wang, Y., Welker, J., Wille, C., Xu, X., Zhang, Z., Zhuang, Q., Zona, D., 2019. Large loss of CO2 in winter observed across the northern permafrost region. Nat. Clim. Chang. 9, 852–857. https://doi.org/10.1038/s41558-019-0592-8.

Olvmo, M., Holmer, B., Thorsson, S., Reese, H., Lindberg, F., 2020. Sub-arctic palsa degradation and the role of climatic drivers in the largest coherent palsa mire complex in Sweden (Vissátvuopmi), 1955–2016. Sci. Rep. 10, 8937. https://doi.org/10.1038/s41598-020-65719-1.

Ortega, J., Helmig, D., 2008. Approaches for quantifying reactive and low-volatility biogenic organic compound emissions by vegetation enclosure techniques – Part A. Chemosphere 72, 343–364. https://doi.org/10.1016/j.chemosphere.2007.11.020.

Peñuelas, J., Staudt, M., 2010. BVOCs and global change. Trends in Plant Science, Special Issue: Induced biogenic volatile organic compounds from plants 15, 133–144. 10.1016/j.tplants.2009.12.005.

Petäjä, T., Tabakova, K., Manninen, A., Ezhova, E., O'Connor, E., Moisseev, D., Sinclair, V.A., Backman, J., Levula, J., Luoma, K., Virkkula, A., Paramonov, M., Räty, M., Äijälä, M., Heikkinen, L., Ehn, M., Sipilä, M., Yli-Juuti, T., Virtanen, A., Ritsche, M., Hickmon, N., Pulik, G., Rosenfeld, D., Worsnop, D.R., Bäck, J., Kulmala, M., Kerminen, V.-M., 2021. Influence of biogenic emissions from boreal forests on aerosol–cloud interactions. Nat. Geosci. 1–6 https://doi.org/10.1038/s41561-021-00876-0.

Ping, C.-L., Michaelson, G.J., Jorgenson, M.T., Kimble, J.M., Epstein, H., Romanovsky, V. E., Walker, D.A., 2008. High stocks of soil organic carbon in the North American Arctic region. Nature Geosci 1, 615–619. https://doi.org/10.1038/ngeo284.

Rinnan, R., Albers, C.N., 2020. Soil uptake of volatile organic compounds: ubiquitous and underestimated? Journal of Geophysical Research: Biogeosciences 125, e2020JG005773. 10.1029/2020JG005773.

Rinnan, R., Gierth, D., Bilde, M., Rosenørn, T., Michelsen, A., 2013. Off-season biogenic volatile organic compound emissions from heath mesocosms: responses to vegetation cutting. Front. Microbiol. 4.

Sannel, A.B.K., Kuhry, P., 2011. Warming-induced destabilization of peat plateau/thermokarst lake complexes. J. Geophys. Res. Biogeo. 116 https://doi.org/10.1029/2010JG001635.

Schade, G.W., Custer, T.G., 2004. OVOC emissions from agricultural soil in northern Germany during the 2003 European heat wave. Atmos. Environ. 38, 6105–6114. https://doi.org/10.1016/j.atmosenv.2004.08.017.

Schmale, J., Zieger, P., Ekman, A.M.L., 2021. Aerosols in current and future Arctic climate. Nat. Clim. Chang. 11, 95–105. https://doi.org/10.1038/s41558-020-00969-5.

Schuur, E. a. G., McGuire, A.D., Schädel, C., Grosse, G., Harden, J.W., Hayes, D.J., Hugelius, G., Koven, C.D., Kuhry, P., Lawrence, D.M., Natali, S.M., Olefeldt, D., Romanovsky, V.E., Schaefer, K., Turetsky, M.R., Treat, C.C., Vonk, J.E., 2015. Climate change and the permafrost carbon feedback. Nature 520, 171–179. 10.1038/nature14338.

Seppälä, M., 1986. The Origin of Palsas. Geografiska Annaler. Series A, Physical Geography 68, 141–147. https://doi.org/10.2307/521453.

Strauss, J., Schirrmeister, L., Wetterich, S., Borchers, A., Davydov, S.P., 2012. Grain-size properties and organic-carbon stock of Yedoma Ice Complex permafrost from the Kolyma lowland, northeastern Siberia. Global Biogeochem. Cycles 26. https://doi.org/10.1029/2011GB004104.

Teufel, B., Sushama, L., 2019. Abrupt changes across the Arctic permafrost region endanger northern development. Nat. Clim. Chang. 9, 858–862. https://doi.org/10.1038/s41558-019-0614-6.

Trowbridge, A.M., Stoy, P.C., Phillips, R.P., 2020. Soil biogenic volatile organic compound flux in a mixed hardwood forest: net uptake at warmer temperatures and the importance of mycorrhizal associations. Journal of Geophysical Research: Biogeosciences 125, e2019JG005479. 10.1029/2019JG005479.

Trucco, C., Schuur, E.A.G., Natali, S.M., Belshe, E.F., Bracho, R., Vogel, J., 2012. Seven-year trends of CO2exchange in a tundra ecosystem affected by long-term permafrost thaw. J. Geophys. Res. Biogeo. 117 https://doi.org/10.1029/2011JG001907.

Turetsky, M.R., Abbott, B.W., Jones, M.C., Walter Anthony, K., Olefeldt, D., Schuur, E.A. G., Koven, C., McGuire, A.D., Grosse, G., Kuhry, P., Hugelius, G., Lawrence, D.M., Gibson, C., Sannel, A.B.K., 2019. Permafrost collapse is accelerating carbon release. Nature 569, 32–34. https://doi.org/10.1038/d41586-019-01313-4.

Turetsky, M.R., Abbott, B.W., Jones, M.C., Anthony, K.W., Olefeldt, D., Schuur, E.A.G., Grosse, G., Kuhry, P., Hugelius, G., Koven, C., Lawrence, D.M., Gibson, C., Sannel, A. B.K., McGuire, A.D., 2020. Carbon release through abrupt permafrost thaw. Nat. Geosci. 13, 138–143. https://doi.org/10.1038/s41561-019-0526-0.

Voigt, C., Marushchak, M.E., Mastepanov, M., Lamprecht, R.E., Christensen, T.R., Dorodnikov, M., Jackowicz-Korczyński, M., Lindgren, A., Lohila, A., Nykänen, H., Oinonen, M., Oksanen, T., Palonen, V., Treat, C.C., Martikainen, P.J., Biasi, C., 2019. Ecosystem carbon response of an Arctic peatland to simulated permafrost thaw. Glob. Chang. Biol. 25, 1746–1764. https://doi.org/10.1111/gcb.14574.

Weidenhamer, J.D., Macias, F.A., Fischer, N.H., Williamson, G.B., 1993. Just how insoluble are monoterpenes? J. Chem. Ecol. 19, 1799–1807. https://doi.org/10.1007/BF00982309.

Wester-Larsen, L., Kramshøj, M., Albers, C.N., Rinnan, R., 2020. Biogenic volatile organic compounds in Arctic soil: a field study of concentrations and variability with vegetation cover. Journal of Geophysical Research: Biogeosciences 125, e2019JG005551. 10.1029/2019JG005551.

Williams, C.J., Yavitt, J.B., 2010. Temperate wetland methanogenesis: The importance of vegetation type and root ethanol production. Soil Sci. Soc. Am. J. 74, 317–325. https://doi.org/10.2136/sssaj2008.0395.

Zhao, J., Wang, Z., Wu, T., Wang, X., Dai, W., Zhang, Y., Wang, R., Zhang, Y., Shi, C., 2016. Volatile organic compound emissions from straw-amended agricultural soils and their relations to bacterial communities: A laboratory study. J. Environ. Sci. 45, 257–269. https://doi.org/10.1016/j.jes.2015.12.036.